Electrochimica Acta 56 (2011) 1432–1438

Contents lists available at ScienceDirect

Electrochimica Acta

journal homepage: www.elsevier.com/locate/electacta

Electrochemical fabrication and potential-enhanced luminescence of $[Ru(bpy)_2tatp]^{2+}$ incorporating DNA-stabilized single-wall carbon nanotubes on an indium tin oxide electrode

Qingyu Guo [a], Jiangyang Shao [a], Ting Sun [b], Hong Li [a,*], Sheng Lan [b], Zhenghe Xu [a]

[a] Key Lab of Technology on Electrochemical Energy Storage and Power Generation in Guangdong Universities, School of Chemistry and Environment, South China Normal University, Guangzhou 510006, PR China
[b] Lab of Photonic Information Technology, School for Information and Optoelectronic Science and Technology, South China Normal University, Guangzhou 510006, PR China

ARTICLE INFO

Article history:
Received 28 June 2010
Received in revised form 23 October 2010
Accepted 26 October 2010
Available online 4 November 2010

Keywords:
Polypyridyl ruthenium(II) complex
DNA
Carbon nanotubes
Electrochemistry
Photoluminescence

ABSTRACT

A simple method was developed for the preparation of $[Ru(bpy)_2tatp]^{2+}$-based aggregates (where bpy = 2,2′-bipyridine, tatp = 1,4,8,9-tetra-aza-triphenylene) on an indium tin oxide (ITO) electrode in the presence of DNA-stabilized single-walled carbon nanotubes (DNA–SWCNTs). The presence of SWCNTs in the concentration range from 0.02 to 0.125 g L^{-1} dispersed with 0.25 mmol L^{-1} DNA was found to promote the immobilization of $[Ru(bpy)_2tatp]^{2+}$ on the ITO electrode by the method of repetitive voltammetric sweeping. The photoluminescence of $[Ru(bpy)_2tatp]^{2+}$ incorporating DNA–SWCNTs both in solution and on the ITO electrode was systematically investigated by emission spectra and fluorescence microscopic imaging. An excess amount of SWCNTs can quench the photoluminescence of $[Ru(bpy)_2tatp]^{2+}$ enhanced by DNA. The anodic potentials combined with CW green laser via an optical microscope was found to significantly increase the emission intensity of $[Ru(bpy)_2tatp]^{2+}$–DNA–SWCNTs aggregates on the ITO electrode. In addition, the electrochemical fabrication and photoluminescence principles of $[Ru(bpy)_2tatp]^{2+}$–DNA–SWCNTs aggregates on the ITO electrode tuned by the external electric fields were discussed in detail.

1. Introduction

Carbon nanotubes (CNTs) have emerged as one of the most extensively studied nanomaterials due to their rich chemical, electrical, optical, and mechanical properties [1,2]. Many research and development efforts have led to a remarkable progress in synthesis, manipulation, functionalization and application of CNTs since the discovery by Iijima in 1991 [3–5]. CNTs have been intensively applied in molecular electronics as field-effect transistors, and in biomedicine as biosensors and drug delivery carriers [6–9]. However, poor dispersion of CNTs in both aqueous and nonaqueous solvents has severely limited their effective uses and further development [10,11]. To adequately disperse CNTs in aqueous solution, various surfactants have been used as dispersants [12,13]. Oligonucleotides helically wrapped around individual CNTs by non-covalent π-stacking interactions between the bases and the CNTs surface, resulting in functionalized CNTs materials [14–16]. The DNA-stabilized CNTs are advantageous for proposed biological applications such as cellular drug delivery, targeted cell destruction and imaging [17–19].

Many ruthenium complexes with polypyridyl ligands possess rich photochemical and photophysical properties, some of them have been fabricated on the CNTs surface by covalent attachment or non-covalent functionalization approaches. For example, $[Ru(bpy)_2(dcbpy)]^{2+}$ (dcbpy = 4,4′-dicarboxy-2,2′-bipyridine) or $[Ru(bpy)_3]^{2+}$ (bpy = 2,2′-bipyridine) was interconnected to the multi-walled CNTs (MWCNTs) for monitoring ammonia in atmosphere or increasing their photoconductivity [20,21]. With tripropylamine as a coreactant, $[Ru(bpy)_3]^{2+}$ on CNTs/Nafion composite films showed sensitive electrochemiluminescence [22,23]. In a previous study, we reported the surfactants-assisted electrochemical immobilization of $[Ru(bpy)_2tatp]^{2+}$ (tatp = 1,4,8,9-tetra-aza-triphenylene) on MWCNTs/glassy carbon electrodes [24]. Synchronously, based on the fortuitous match between the redox potentials of polypyridyl Ru(III) complexes with DNA, some of them have been used as the mediators for the oxidation of DNA or DNA-wrapped CNTs. Thorp and his coauthors showed an electrochemical oxidation of DNA-wrapped CNTs by electrogenerated $[ML_3]^{3+}$ (M = Ru(III), Os(III) and Fe(III); L = 2,2′-bipyridine or 4,4′-dimethyl-2,2′-bipyridine) [25,26]. According to the redox-controlled luminescence properties of Ru(II) complexes, they can

* Corresponding author. Tel.: +86 20 39310068; fax: +86 20 39310187.
E-mail address: lihong@scnu.edu.cn (H. Li).

0013-4686/$ – see front matter © 2010 Elsevier Ltd. All rights reserved.
doi:10.1016/j.electacta.2010.10.064

indicate the damage of DNA and photo-induced electron transfer through DNA [27].

CNTs play profound roles as matrix to immobilize polypyridyl ruthenium complexes and as promoter to accelerate the electron transfer with the substrate electrodes [28]. The metal-mediated or photoinduced electron transfer of CNTs increases the number of charge carriers (either electrons or holes), which results in an enhancement of CNTs conductance and obtains the potential applications to chemical and biological sensing [29,30]. Synchronously, CNTs have shown superior quenching efficiency toward a variety of organic fluorophores or fluorophore-labeled DNA [31], therefore the uses of CNTs have the potential to indicate the delivery of DNA or drugs as well as the dissociation of DNA-CNTs [32].

In the present work, our interest is focused on the fabrication of polypyridyl ruthenium(II) complex $[Ru(bpy)_2tatp]^{2+}$ associated with DNA-stabilized CNTs on solid electrodes via a solid–liquid interface and the electrochemically tuned luminescence of $[Ru(bpy)_2tatp]^{2+}$ incorporating DNA-stabilized CNTs. Similar to the DNA-enhanced immobilization of several polypyridyl ruthenium(II) complexes on an ITO electrode reported by our previous papers [33,34], the presence of SWCNTs stabilized by DNA can promote the electrochemical immobilization of $[Ru(bpy)_2tatp]^{2+}$ on the ITO electrode using a simple method of repetitive voltammetric sweeping. Although the photoluminescence of $[Ru(bpy)_2tatp]^{2+}$–DNA aggregates on the ITO surface is quenched by SWCNTs, the electrochemically tuned luminescence of $[Ru(bpy)_2tatp]^{2+}$–DNA–SWCNTs aggregates on the ITO electrode is enhanced by increasing anodic potentials.

2. Experimental

2.1. Chemicals and materials

Tris-hydroxy methyl amino-methane (Tris) from Sigma Chemical Company was used to prepare electrolyte buffer solutions. The single-walled carbon nanotubes (SWCNTs) with the inside diameter of 2–5 nm and the length of 10–30 μm was obtained from Chengdu Organic Chemistry Co., Ltd., China. Calf thymus DNA (Huamei Co., China) and sodium dodecylsulfate (SDS) were used as received. Unless otherwise noted, the buffer solution was 10 mmol L^{-1} Tris/50 mmol L^{-1} NaCl of pH 7.2, prepared with doubly distilled water. $[Ru(bpy)_2tatp]Cl_2$ and $[Ru(bpy)_2dppz]Cl_2$ were synthesized following procedures reported previously [35–37]. The structure of $[Ru(bpy)_2tatp]^{2+}$ is shown in Fig. 1a. The DNA-stabilized SWCNT suspensions with 0.1 mmol L^{-1} $[Ru(bpy)_2tatp]^{2+}$ were prepared by dispersing a desired amount of SWCNTs into Tris buffer solutions containing 0.25 mmol L^{-1} DNA with the aid of ultrasonic agitation of 200 W power for ca. 40 min. As shown in Fig. 1b, the SWCNTs has been effectively dispersed by the introduction of DNA and the $[Ru(bpy)_2tatp]^{2+}$–DNA-CNTs in aqueous solution is stable.

2.2. Methods and experimental conditions

Voltammetric measurement was performed on a CHI660a electrochemical system (Shanghai, China) in a regular three-electrode cell with 0.4 mL test solution. An indium tin oxide (ITO) was used as the working electrode (20 Ω cm^{-2}, Shenzhen Nanbo Co. Ltd, China), while platinum plate was used as counter electrode and Ag-AgCl (50 mmol L^{-1} NaCl) as reference electrode, showing a potential of 0.3058 V *versus* a standard hydrogen electrode (SHE).

Steady-state emission spectra were recorded using a RF-2500 fluorescent spectrometer. The samples were excited at 450 nm. The fluorescence image was taken using a Nikon Eclipse TS100 inverted fluorescence microscope (Japan), equipped with a 50 W mercury lamp. The images were captured with a Nikon E4500 camera with blue light radiation.

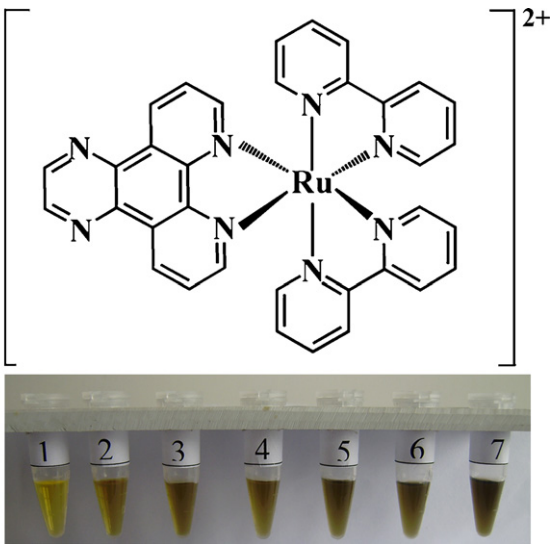

Fig. 1. (a) Structure of $[Ru(bpy)_2tatp]^{2+}$, (b) Photographs of the SWCNTs suspension stabilized with 0.25 mmol L^{-1} DNA in the presence of 0.1 mmol L^{-1} $[Ru(bpy)_2tatp]^{2+}$. The mass concentration of SWCNTs (g L^{-1}): (1) 0, (2) 0.020, (3) 0.031, (4) 0.042, (5) 0.063, (6) 0.094, and (7) 0.125.

Potential-enhanced emission spectra were recorded using a home-built system, consisting of an optical microscope (Zeiss Axio Observer A1, Germany) and a CW green laser source (Coherent Verdi-5, USA), interfaced with an electrochemical system. A laser beam was reflected by a dichroscope. The reflected beam was focused on the surface of desired depth in the working electrode through an objective lens. The emission spectra were collected using the same objective lens to direct the emitted beam from the sample through the dichroscope, followed by a low-pass filter and a grating spectrometer (7ISW3052, Beijing, China) to a photo multiplier tube (PMT 7ID101-CR131, Beijing, China).

All the experiments were performed at room temperatures (23–25 °C).

3. Results and discussion

3.1. Electrochemical fabrication of $[Ru(bpy)_2tatp]^{2+}$ incorporating DNA-stabilized CNTs on the ITO electrode

3.1.1. Electrochemistry controlled by diffusion process

The repetitive differential pulse voltammograms (DPVs) of $[Ru(bpy)_2tatp]^{2+}$ in the presence of DNA–SWCNTs are shown in Fig. 2. In this figure, an anodic wave at 1.041 V, labeled as wave I, is observed. Since a similar anodic peak was previously reported for $[Ru(bpy)_3]^{2+}$ [38], the anodic wave is assigned to the oxidation of soluble Ru(II) to Ru(III). After 21 differential pulse voltammetric scans, the effect of scan rate on the electrochemical behavior of $[Ru(bpy)_2tatp]^{2+}$ in the presence of 0.25 mmol L^{-1} DNA/0.125 g L^{-1} SWCNTs on the ITO electrode is studied. The results in Fig. 3 show an anodic ($E_{p,a}$) and a cathodic ($E_{p,c}$) peak at 1.107 V and 0.999 V, respectively, with a peak separation, ΔE_p of 108 mV and a formal potential, $E^{\circ\prime}$ of 1.053 V, taken as the half of the sum of $E_{p,a}$ and $E_{p,c}$. The current ratio of anodic peak to cathodic peak was close to 1 for all the scan rates, while the peak current was proportional to the square root of scan rate ($\upsilon^{1/2}$) over the scan rate range from 0.05 to 0.5 V s^{-1} (inset a). In the absence of DNA–SWCNTs, as shown in Fig. 4, $[Ru(bpy)_2tatp]^{2+}$ (curve 1) indicates a similar response. According to these results, it is suggested that the Ru(III)/Ru(II) reaction (wave I) in the presence of DNA–SWCNTs conforms to

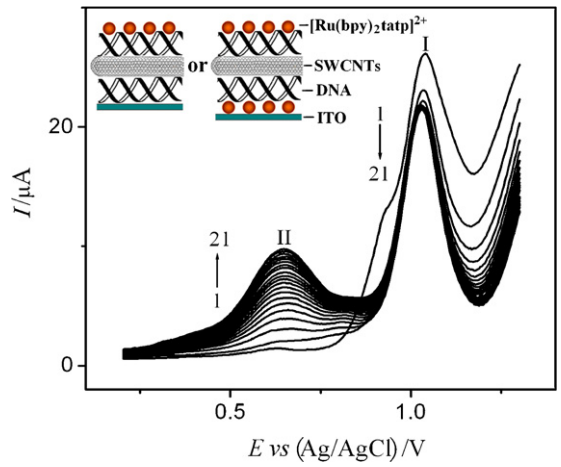

Fig. 2. Progressive DPVs of 0.1 mmol L^{-1} $[Ru(bpy)_2tatp]^{2+}$ on the ITO electrode in the presence of 0.25 mmol L^{-1} DNA/0.125 g L^{-1} SWCNTs. The inset shows the assembled principle of $[Ru(bpy)_2tatp]^{2+}$ incorporating DNA-stabilized SWCNTs on the surface.

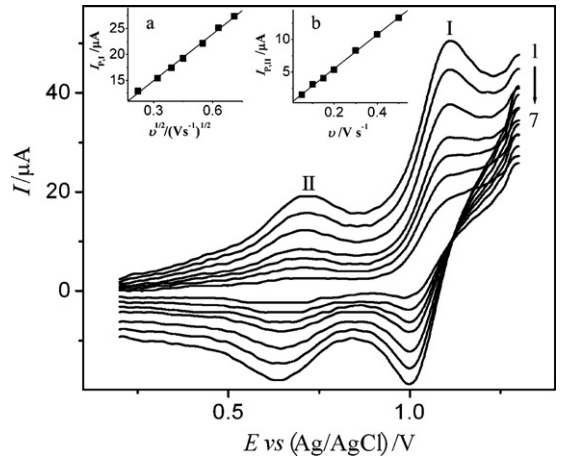

Fig. 3. CVs of 0.1 mmol L^{-1} $[Ru(bpy)_2tatp]^{2+}$ on the ITO electrode in the presence of 0.25 mmol L^{-1} DNA/0.125 g L^{-1} SWCNTs after differential pulse voltammetric sweeping of 21 cycles. Scan rate (V s^{-1}): (1) 0.5, (2) 0.4, (3) 0.3, (4) 0.2, (5) 0.15, (6) 0.10, (7) 0.05. The insets a and b show the relation of peak I current *versus* the square root of scan rate and peak II current *versus* scan rate, respectively.

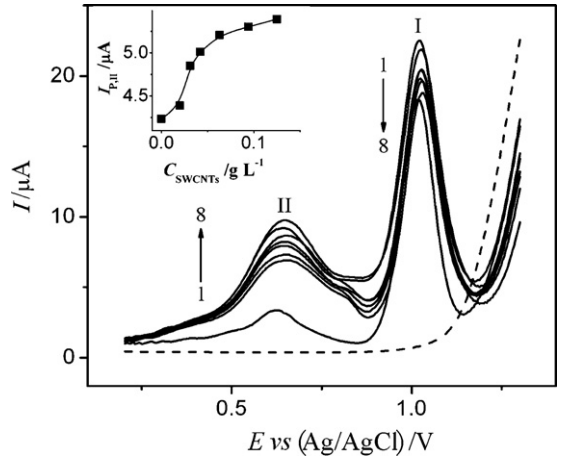

Fig. 4. The 21st DPVs of 0.1 mmol L^{-1} $[Ru(bpy)_2tatp]^{2+}$ on the ITO electrode in the absence (line 1) and presence of 0.25 mmol L^{-1} DNA and different concentration SWCNTs (g L^{-1}): (2) 0, (3) 0.020, (4) 0.031, (5) 0.042, (6) 0.063, (7) 0.094, (8) 0.125. The dashed line represents the 21st DPV of 0.20 mmol L^{-1} DNA/0.05 g L^{-1} SWCNTs. The inset corresponds to peak II current *versus* SWCNTs concentration.

reversible characteristics and DNA–SWCNTs effectively mediate the electron transfer between Ru(II) species and ITO surface [39].

3.1.2. Electrochemistry controlled by surface adsorption process

More interestingly, when voltammetric sweeping was carried out over the potential range from 0.2 to 1.3 V in the presence of DNA–SWCNTs, as seen in Fig. 2, a new wave (II) is observed at 0.640 V. The peak II currents increase with increasing voltammetric sweeping number. After 21 differential pulse voltammetric scans, the voltammograms in Fig. 3 not only show a scan rate-dependent ΔE_p, but also peak II currents linearly increase with the rise of scan rate. These electrochemical characteristics indicate that the $[Ru(bpy)_2tatp]^{2+}$-based species with excellent redox activities are immobilized on the ITO surface.

When continuous voltammetric sweeping was carried out in the absence of DNA–SWCNTs, as shown in curve 1 of Fig. 4, the current of peak II is much smaller than that in the presence of DNA–SWCNTs, suggesting that the presence of DNA–SWCNTs promotes the immobilization of $[Ru(bpy)_2tatp]^{2+}$ on ITO surfaces. For a fixed concentration of DNA at 0.25 mmol L^{-1}, with the rise of SWCNTs concentrations, an increasing amount of $[Ru(bpy)_2tatp]^{2+}$ appears to be immobilized on ITO surfaces, as shown by an increased current intensity of anodic peak II (curves 1–8). These results encourage us to use DNA-stabilized SWCNTs as bridges for fabricating a multifunctional biomolecular film containing nanomaterials and surface-confined redox centers of controllable thickness by electrochemical deposition method.

It is worthy to note that the peak II potentials both in the absence and presence of DNA–SWCNTs display a negative shift of about 0.383 ± 0.010 V compared to that of peak I. The anodic current of peak II is nearly equal to the cathodic peak for all the scan rates (Fig. 3). These results imply that the peak II could be ascribed to adsorption-controlled reactions of Ru(II)-based species. To illustrate the peak II reaction, several electrochemical experiments are involved and the corresponding analysis is as follows: (i) in the potential range from 0.2 to 1.3 V, as seen by the dashed line in Fig. 4, no anodic wave of DNA or guanine is observed and hence the DNA–SWCNTs is basically stable in our experimental conditions. (ii) The presence of sodium dodecylsulfate (SDS) effectively increases the peak II current as shown in Fig. 5, revealing that the formation of peak II in the presence of DNA–SWCNTs is mainly dependent on the polyanion structure of DNA, rather than the oxidation of guanine in DNA. Of course, an appropriate amount of guanine also increases the peak II height of Ru(II) complexes reported by our previous paper [40]. (iii) When the ITO electrode is altered into a glassy carbon (GC) electrode, as depicted in Fig. 6, only a pair of diffusion-controlled waves (peak I) is observed and the peak II is absent on the GC surface. This result suggests that the geometric and electric structure characteristics of ITO facilitate the emergence of peak II. (iv) In our previous studies [41], it has been found that the CVs for an anisomerous ruthenated porphyrin $[Ru(MPyTPP)(bpy)_2Cl]^+$ (where bpy = 2,2′-bipyridine, MPyTPP = 5-pyridyl-10,15,20-triphenyl porphyrin) only present a pair of surface-controlled redox waves. However, $[Ru(bpy)_3]^{2+}$ shows a very different case, only a pair of diffusion-controlled waves (peak I) is observed. This finding implies that the peak II reaction of $[Ru(bpy)_2tatp]^{2+}$ on ITO electrodes is influenced by the component and structure of Ru(II) complexes. The extended π-conjugated planar area and two nitrogen atoms with lone pairs in $[Ru(bpy)_2tatp]^{2+}$ facilitate the formation of peak II.

From what has been discussed above, the peak II is ascribed to the $[Ru(bpy)_2tatp]^{3+/2+}$ reaction immobilized on the ITO electrode in the process of voltammetric sweeping. The dissolved Ru(II) reactant is oxidized to form a layer of Ru(III)-based product adsorbed strongly on ITO electrodes and hence the peak II is considered as a prewave [33,34]. The surface coverage of

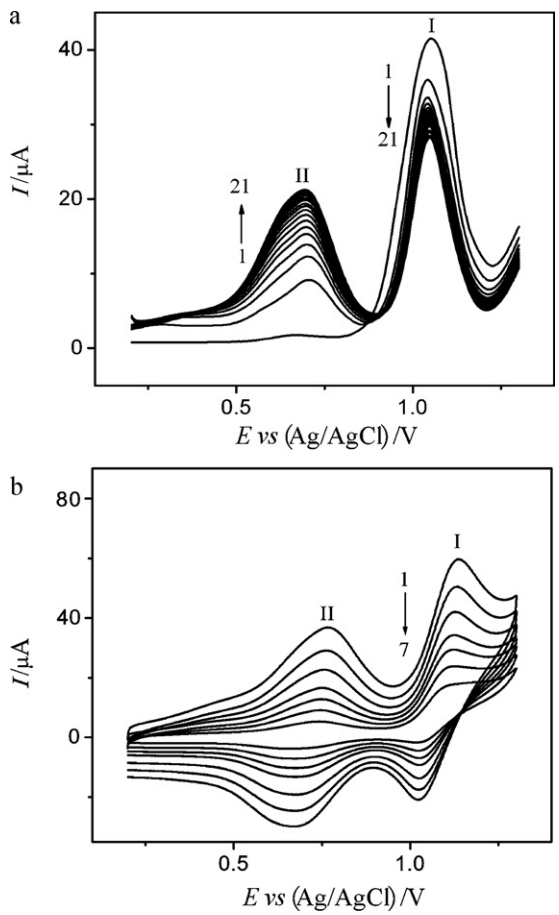

Fig. 5. Progressive DPVs (a) and CVs (b) of 0.1 mmol L^{-1} $[Ru(bpy)_2tatp]^{2+}$ in the presence of 0.20 mmol L^{-1} SDS on the ITO electrode. Scan rate (V s^{-1}): (1) 0.5, (2) 0.4, (3) 0.3, (4) 0.2, (5) 0.15, (6) 0.10, (7) 0.05.

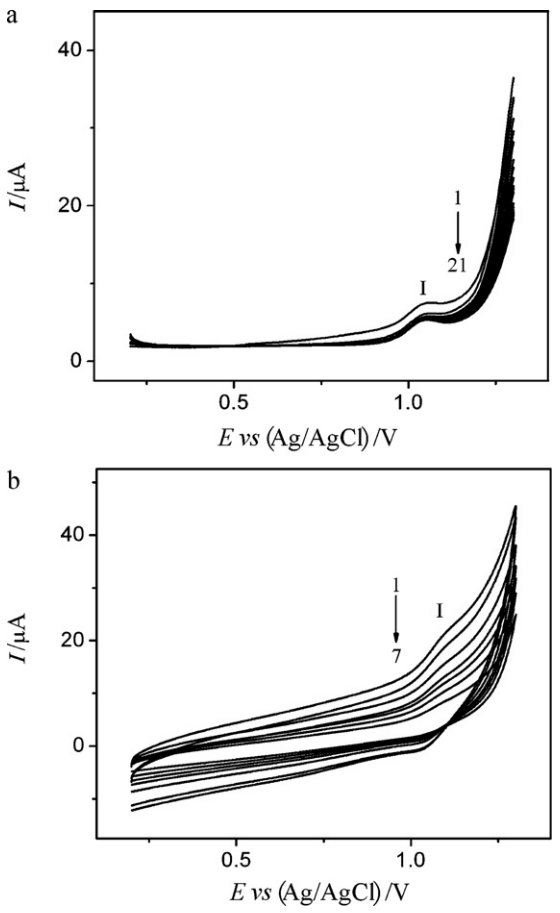

Fig. 6. Progressive DPVs (a) and CVs (b) of 0.1 mmol L^{-1} $[Ru(bpy)_2tatp]^{2+}$ on the GC electrode. Scan rate (V s^{-1}): (1) 0.5, (2) 0.4, (3) 0.3, (4) 0.2, (5) 0.15, (6) 0.10, (7) 0.05.

$[Ru(bpy)_2tatp]^{2+}$-based adsorption is estimated by the slope of the inset in Fig. 3, which is 3.5×10^{-11} mol cm^{-2} [39]. The value suggests that the adsorbed $[Ru(bpy)_2tatp]^{2+}$ in the presence of DNA–SWCNTs corresponds to a sub-monolayer [42]. Combined with the results revealed by the latter emission spectra and fluorescence microscopic images, $[Ru(bpy)_2tatp]^{2+}$–DNA–SWCNTs aggregates were formed due to interactions between positively charged $[Ru(bpy)_2tatp]^{2+}$ and negatively charged DNA–SWCNTs in solution and hence $[Ru(bpy)_2tatp]^{2+}$ is proposed to mainly bind with DNA, rather than SWCNTs. Thus, as depicted in the inset of Fig. 2, DNA–SWCNTs may act as the bridge to promote the adsorption of $[Ru(bpy)_2tatp]^{3+/2+}$ on ITO surfaces by electrostatic attraction and hydrophobic interaction. Consequently, the presence of DNA–SWCNTs in turn enhances the oxidation of Ru(II) species to the adsorbed Ru(III) species and the peak II height shows a gradual increase in the subsequent voltammetric sweeping.

3.2. Photoluminescence of $[Ru(bpy)_2tatp]^{2+}$ incorporating DNA-stabilized CNTs

Fig. 7 shows the emission spectra of soluble $[Ru(bpy)_2tatp]^{2+}$ in the absence and presence of DNA-stabilized SWCNTs. In the absence of DNA-stabilized SWCNTs (curve 1), an intense emission peak at 601 nm is observed. This emission peak is attributed to the d–π* electron transition from Ru(II)-to-ligand [43]. The addition of 0.035 mmol L^{-1} DNA without SWCNTs leads to a significant enhancement of the luminescence without a noticeable shift in peak position, attributed to the conjugation of $[Ru(bpy)_2tatp]^{2+}$ with DNA by intercalating into the bases of DNA with tatp ligand (curve 2) [44,45]. In the presence of both DNA and SWCNTs, however, the luminescence of $[Ru(bpy)_2tatp]^{2+}$ enhanced by 0.035 mmol L^{-1} DNA is progressively reduced with increasing the concentration of SWCNTs as shown by spectra 3,4 and 5 in Fig. 7. In the presence of 1.46 mg L^{-1} SWCNTs and 0.035 mmol L^{-1} DNA, the luminescence intensity is decreased by 38.5% of the case without SWCNTs. This finding suggests the $[Ru(bpy)_2tatp]^{2+}$–DNA–SWCNTs aggregates may be formed by interactions among $[Ru(bpy)_2tatp]^{2+}$, DNA and SWCNTs. It is possible due to SWCNTs as an effective

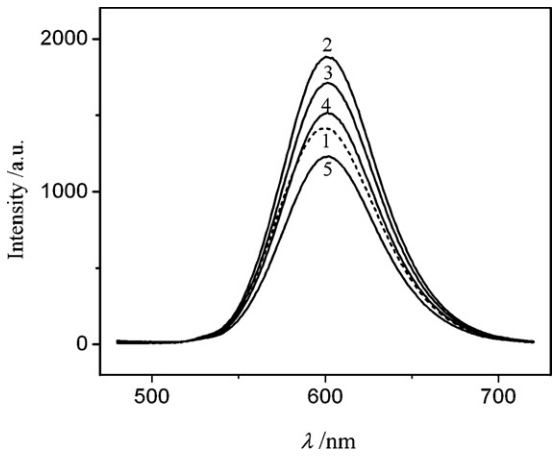

Fig. 7. Emission spectra of 0.01 mmol L^{-1} $[Ru(bpy)_2tatp]^{2+}$ in the absence (dashed line 1) and presence of 0.035 mmol L^{-1} DNA and different concentration SWCNTs (mg L^{-1}): (2) 0, (3) 0.36, (4) 0.73, (5) 1.46.

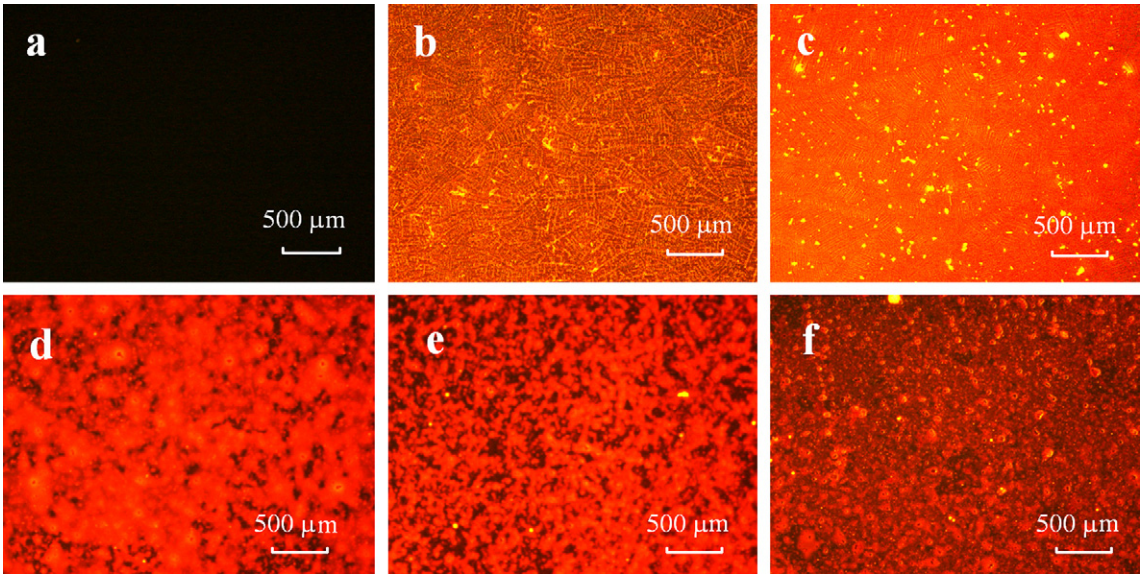

Fig. 8. Fluoresence microscopic images of ITO (a) and 0.1 mmol L^{-1} $[Ru(bpy)_2tatp]^{2+}$ on the ITO surface in the absence (b) and presence of 0.25 mmol L^{-1} DNA and SWCNTs (g L^{-1}) (c) 0, (d) 0.031, (e) 0.063, (f) 0.094.

quencher [31], the luminescence intensity of $[Ru(bpy)_2tatp]^{2+}$ in the presence of DNA decreases with increasing SWCNT concentration.

In order to further illustrate the formation of $[Ru(bpy)_2tatp]^{2+}$–DNA–SWCNTs aggregates and to avoid the quenching of Ru(II)-based excited state luminescence by solvent water molecules, a given mass of $[Ru(bpy)_2tatp]^{2+}$ associated with DNA–SWCNTs is immobilized onto an ITO surface by solution cast method, i.e., placing the $[Ru(bpy)_2tatp]^{2+}$–DNA–SWCNTs suspension drop-wise on the ITO surface, followed by solvent evaporation/drying at room temperature. As depicted by Fig. 8, the fluorescence image of $[Ru(bpy)_2tatp]^{2+}$ in the absence of DNA and SWCNTs on the ITO surface shows an intense orange–red appearance under the excitation of blue light, in contrast to a black appearance of ITO surface. The brightness of orange–red appearance increases significantly when $[Ru(bpy)_2tatp]^{2+}$ is cast on the ITO surface in the presence of 0.25 mmol L^{-1} DNA or 0.031 g L^{-1} SWCNTs/0.25 mmol L^{-1} DNA, indicating an enhanced luminescence of $[Ru(bpy)_2tatp]^{2+}$, although the appearance is less uniform with sporadic black areas in the presence of 0.031 g L^{-1} SWCNTs. With increasing SWCNTs concentrations from 0.031 g L^{-1} to 0.094 g L^{-1}, the fluorescence images show a decreased area of bright orange–red appearance with progressively more dark areas, suggesting that the luminescence of $[Ru(bpy)_2tatp]^{2+}$ is promoted by DNA, and the presence of SWCNTs decreases the luminescence $[Ru(bpy)_2tatp]^{2+}$ enhanced by DNA. This result is in excellent agreement with the observations in Fig. 7, revealing that $Ru(bpy)_2tatp]^{2+}$–DNA–SWCNTs aggregates are formed both in solution and on the ITO surface. More importantly, it provides an effective to modulate the photoluminescence of $[Ru(bpy)_2tatp]^{2+}$ by DNA and SWCNTs.

3.3. *Luminescence of $[Ru(bpy)_2tatp]^{2+}$–DNA–SWCNTs aggregates enhanced by anodic potentials*

With the encouraging results above, an attempt was made to fabricate a photoluminescence film with SWCNTs and biomolecules tuned by in situ electrochemical method. The presence of DNA-stabilized SWCNTs is shown to influence the electrochemical immobilization and luminescence properties of $[Ru(bpy)_2tatp]^{2+}$ on ITO electrodes. It is therefore interesting to investigate whether the photoluminescence of Ru(II)–DNA–SWCNTs aggregates could be modulated by the applied electrode potentials. Fig. 9a shows the emission spectra of $[Ru(bpy)_2tatp]^{2+}$–DNA–SWCNTs aggregates immobilized on ITO electrodes under varying anodic potentials. Under the excitation of CW green laser, a broad emission peak at 624 nm was observed for all the cases. The varying anodic potentials did not cause any noticeable shift in the position of emission peak, implying that the species responsible for the excitation is identical and hence the chemical nature of the aggregates is independent of applied external electric fields. However, the luminescence intensity is significantly enhanced as the applied electrode potential increases. For example, an applied electrode potential of 1.2 V above the open circuit potential increased the luminescence intensity by 296%. This finding reveals that the photoluminescence of $[Ru(bpy)_2tatp]^{2+}$–DNA–SWCNTs aggregates can be finely tuned by the external electrode potentials.

When the green laser is turned off, the application of 1.2 V anodic potential does not lead to a detectable luminescent signal on ITO electrodes under our experimental conditions, as shown by the dashed line of Fig. 9a. It is clear that the contribution of electroluminescence (or electrochemiluminescence) under 1.2 V applied electrode potential in the absence of laser is too low to be detected by our PMT. It is interesting to note that for this system, the luminescence intensity excited by green laser increases linearly with increasing applied electrode potentials as shown in the inset of Fig. 9a. This linear relationship suggests the direct effect of applied electrode potentials on the excited species under the irradiation of green laser. To explain this finding, Fig. 9a′ shows the luminescence principle of $[Ru(bpy)_2tatp]^{2+}$–DNA–SWCNTs aggregates tuned by the external electric fields. When anodic potentials are applied to the working electrode, holes generated from the ITO electrode are injected into the Ru(II)-based layer. Under the irradiation of green laser, the excited state of Ru(II)-based aggregates releases electrons. As the binding energy of electrons with holes is large enough, they recombine to yield excitons [46,47]. Consequently, the luminescence intensity of $[Ru(bpy)_2tatp]^{2+}$–DNA–SWCNTs aggregates is enhanced by the external electric fields.

In order to further illustrate how the external electric fields influence the luminescence of $[Ru(bpy)_2tatp]^{2+}$-based species, another classical Ru(II) complex $[Ru(bpy)_2dppz]^{2+}$ (dppz = dipyrido[3,2-*a*:2′,3′-*c*]phenazine) is used for a comparison. Fig. 9b shows the emission spectra of $[Ru(bpy)_2dppz]^{2+}$–DNA–SWCNTs aggregates immobilized on

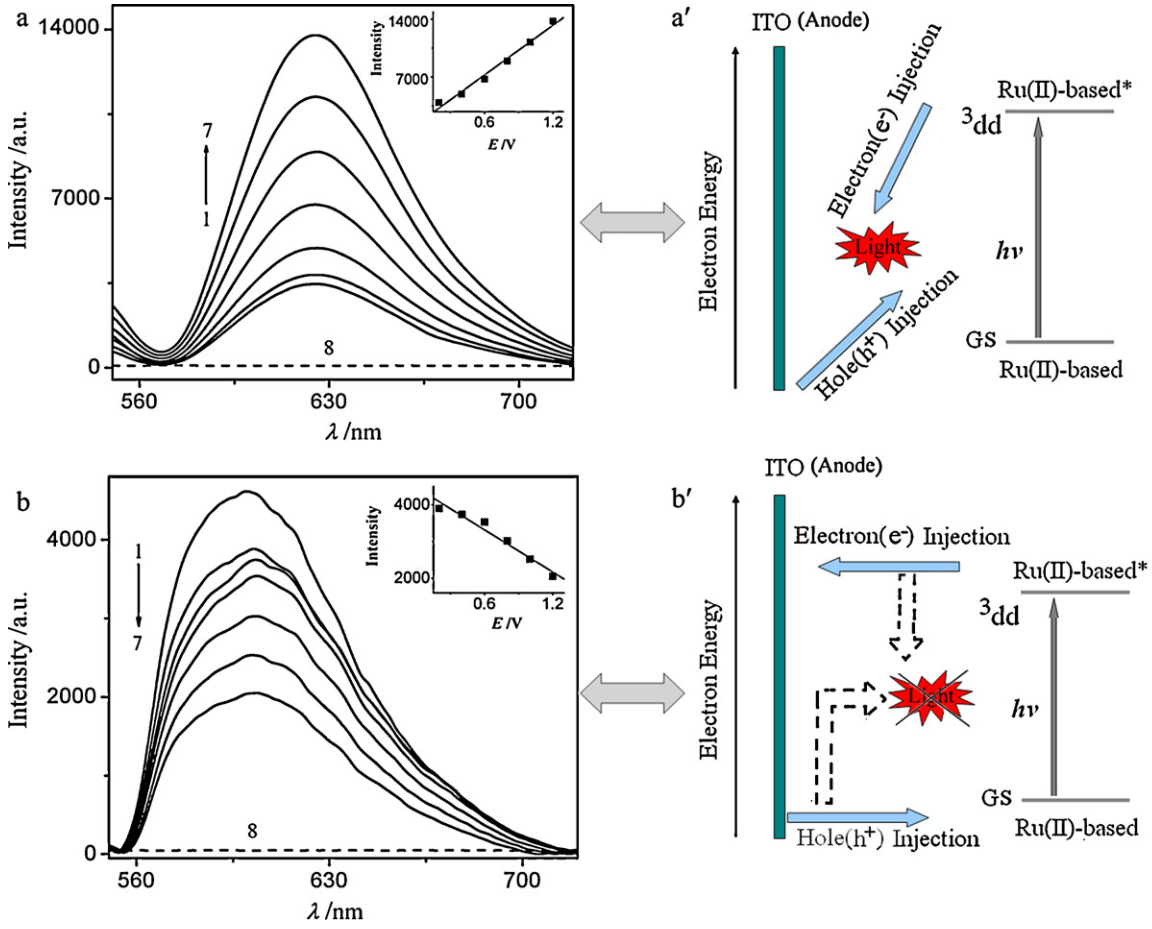

Fig. 9. Emission spectra of $[Ru(bpy)_2tatp]^{2+}$–DNA–SWCNTs (a) and $[Ru(bpy)_2dppz]^{2+}$–DNA–SWCNTs (b) on the ITO electrode in buffer solution at the excitation of CW green laser tuned by anodic potentials *E versus* (Ag/AgCl)/V: (1) open circuit potential, (2) 0.2, (3) 0.4, (4) 0.6, (5) 0.8, (6) 1.0, (7) 1.2. PMT biased voltage: −460 V, modulated sensitivity: 2 mV. The dashed line 8 corresponds to the emission spectroscopy in the absence of CW green laser at an applied potential of 1.2 V. The inset shows the luminescence intensity as a function of *E*. The schematic diagrams a′ and b′ show the luminescence principles corresponding to spectra a and b, respectively.

ITO electrodes under the excitation of laser as the anodic potential increases. Interestingly, the luminescence intensity of $[Ru(bpy)_2dppz]^{2+}$-based aggregates shows a linear decrease with increasing anodic potentials. This result implies that the excited state luminescence of $[Ru(bpy)_2dppz]^{2+}$–DNA–SWCNTs aggregates is quenched by the external electric fields, which differs from that of $[Ru(bpy)_2tatp]^{2+}$-based aggregates. It is well-known that although dppz ligand has a more extended π-conjugated ligand in contrast to tatp, $[Ru(bpy)_2dppz]^{2+}$ exhibits a negligible emission in water and the photoluminescence efficiency (quantum yield) is very small arising from a $d(Ru) \rightarrow \pi^*(dppz)$ electron transition [48]. Thus, the binding energy of electrons with holes may be too weak to recombine for yielding excitons. As depicted by Fig. 9b′, when anodic potentials are applied to the working electrode modified with $[Ru(bpy)_2dppz]^{2+}$–DNA–SWCNTs aggregates, holes generated from the ITO electrode are flowed into the Ru(II)-based layer, however the electrons from the excited state of Ru(II)-based aggregates are flowed into the ITO electrode under the irradiation of green laser. So the luminescence intensity of $[Ru(bpy)_2dppz]^{2+}$–DNA–SWCNTs aggregates is decreased by the external electric fields.

4. Conclusions

A simple technique based on repetitive voltammetric sweeping has been developed for controllable immobilization of polypyridyl Ru(II) complexes promoted by DNA-stabilized SWCNTs on ITO electrodes. With this technique, a biomolecular film with surface-confined redox center and luminescence properties is fabricated. Furthermore, the anodic potentials combined with CW green laser via an optical microscope is applied to study the luminescence of $[Ru(bpy)_2tatp]^{2+}$–DNA–SWCNTs aggregates immobilized on ITO electrodes in buffer solution. From this study, the following conclusions are derived.

(1) In the absence and presence of DNA-stabilized SWCNTs, a pair of diffusion-controlled waves and a pair of surface-controlled waves are observed on cyclic voltammograms of $[Ru(bpy)_2tatp]^{2+}$-based species. The presence of DNA–SWCNTs is found to promote the electrochemical immobilization of $[Ru(bpy)_2tatp]^{3+/2+}$ on ITO electrodes.
(2) An excess amount of SWCNTs quenches the luminescence of $[Ru(bpy)_2tatp]^{2+}$ enhanced by DNA.
(3) The emission intensity of $[Ru(bpy)_2tatp]^{2+}$–DNA–SWCNTs aggregates on the ITO electrode is promoted by increasing applied electrode potentials under the excitation of CW green laser. DNA-stabilized SWCNTs can effectively mediate the photo-induced electron transfer between $[Ru(bpy)_2tatp]^{2+}$-based species and ITO surface.

Acknowledgements

We are grateful to the Specialized Research Fund for the Doctoral Program of Higher Education of China (No. 20094407120008) for their financial support.

References

[1] R.L. McCreery, Chem. Rev. 108 (2008) 2646.
[2] M.S. Mauter, M. Elimelech, Environ. Sci. Technol. 42 (2008) 5643.
[3] S. Iijima, Nature 354 (1991) 56.
[4] Y.L. Zeng, Y.F. Huang, J.H. Jiang, X.B. Zhang, C.R. Tang, G.L. Shen, R.Q. Yu, Electrochem. Commun. 9 (2007) 185.
[5] G.H. Xu, Q. Zhang, J.Q. Huang, M.Q. Zhao, W.P. Zhou, F. Wei, Langmuir 26 (2010) 2798.
[6] G. Gruner, Anal. Bioanal. Chem. 384 (2006) 322.
[7] K. Balasubramanian, M. Burghard, Anal. Biochem. 385 (2006) 452.
[8] S.N. Kim, J.F. Rusling, F. Papadimitrakopoulos, Adv. Mater. 19 (2007) 3214.
[9] F.S. Lu, L.R. Gu, M.J. Meziani, X. Wang, P.J. Luo, L.M. Veca, L. Cao, Y.P. Sun, Adv. Mater. 21 (2009) 139.
[10] V.A. Sinani, M.K. Gheith, A.A. Yaroslavov, A.A. Rakhnyanskaya, K. Sun, A.A. Mamedov, J.P. Wicksted, N.A. Kotov, J. Am. Chem. Soc. 127 (2005) 3463.
[11] Y. Maeda, S. Kimura, Y. Hirashima, M. Kanda, Y. Lian, T. Wakahara, T. Akasaka, T. Hasegawa, H. Tokumoto, T. Shimizu, H. Kataura, Y. Miyauchi, S. Maruyama, K. Kobayashi, S. Nagase, J. Phys. Chem. B 108 (2004) 18395.
[12] A. Erdem, P. Papakonstantiou, H. Murphy, Anal. Chem. 78 (2006) 6656.
[13] J.X. Gao, J.F. Rusling, J. Electroanal. Chem. 449 (1998) 1.
[14] M. Zheng, A. Jagota, E.D. Semke, B.A. Diner, R.S. McLean, S.R. Lustig, R.E. Richardson, N.G. Tassi, Nat. Mater. 2 (2003) 338.
[15] M.E. Hughes, E. Brandin, J.A. Golovchenko, Nano Lett. 7 (2007) 1191.
[16] J.F. Campbell, I. Tessmer, H.H. Thorp, D.A. Erie, J. Am. Chem. Soc. 130 (2008) 10648.
[17] M.L. Becker, J.A. Fagan, N.D. Gallant, B.J. Bauer, V. Bajpai, E.K. Hobbie, S.H. Lacerda, K.B. Migler, J.P. Jakupciak, Adv. Mater. 19 (2007) 939.
[18] Z. Liu, M. Winters, M. Holodniy, H. Dai, Angew. Chem. Int. Ed. 46 (2007) 2023.
[19] P. Cherukuri, S.M. Bachillo, S.H. Litovsky, R.B. Weisman, J. Am. Chem. Soc. 126 (2004) 15638.
[20] F. Frehill, J.G. Vos, S. Benrezzak, A.A. Koós, Z. Kónya, M.G. Rüther, W.J. Blau, A. Fonseca, J.B. Nagy, L.P. Biró, A.I. Minett, M. in het Panhuis, J. Am. Chem. Soc. 124 (2002) 13694.
[21] R.F. Khairoutdinov, L.V. Doubova, R.C. Haddon, L. Saraf, J. Phys. Chem. B 108 (2004) 19976.
[22] Z. Guo, S. Dong, Anal. Chem. 76 (2004) 2683.
[23] M.M. Richter, Chem. Rev. 104 (2004) 3003.
[24] W.Y. Zou, L. Wang, B.Y. Lu, H. Li, H.Y. Chen, J. Appl. Electrochem. 39 (2009) 2015.
[25] M.E. Napier, D.O. Hull, H.H. Thorp, J. Am. Chem. Soc. 127 (2005) 11952.
[26] F.J. Campbell, M.E. Napier, S.W. Feldberg, H.H. Thorp, J. Phys. Chem. B 114 (2010) 8861.
[27] H. Ali, J.E. van Lier, Chem. Rev. 99 (1999) 2379.
[28] L. Zhang, S. Dong, Electrochem. Commun. 8 (2006) 1687.
[29] M. Zheng, V.V. Rostovtsev, J. Am. Chem. Soc. 128 (2006) 7702.
[30] S. Boussaad, B.A. Diner, J. Fan, J. Am. Chem. Soc. 130 (2008) 3780.
[31] Z. Zhu, R.H. Yang, M.X. You, X.L. Zhang, Y.R. Wu, W.H. Tan, Anal. Bioanal. Chem. 396 (2010) 73.
[32] R.H. Yang, Z.W. Tang, J.L. Yan, H.Z. Kang, Y. Kim, Z. Zhu, W.H. Tan, Anal. Chem. 80 (2008) 7408.
[33] H. Li, Z. Xu, D.W. Pang, J.Z. Wu, L.N. Ji, Z.H. Lin, Electrochim. Acta 51 (2006) 1996.
[34] H. Li, Y.J. Liu, J. Xu, Z. Xu, L.N. Ji, W.S. Li, H.Y. Chen, Electrochim. Acta 52 (2007) 4956.
[35] L.A. Zwelling, S. Michaels, H. Schwartz H, P.P. Dobson, K.W. Kohn, Cancer Res. 41 (1981) 640.
[36] A.E. Friedman, J.C. Chambron, J.P. Sauvage, N.J. Turro, J.K. Barton, J. Am. Chem. Soc. 112 (1990) 4960.
[37] R.M. Hartshorn, J.K. Barton, J. Am. Chem. Soc. 114 (1992) 5919.
[38] X.X. Yan, H. Li, Z. Xu, W.S. Li, Bioelectrochemistry 74 (2009) 310.
[39] A.J. Bard, L.R. Faulkner, Electrochemical Methods, Wiley, New York, 1980.
[40] W. Hong, H. Li, S. Yao, F. Sun, Z. Xu, Electrochim. Acta 54 (2009) 3250.
[41] H. Li, W.J. Mei, Z. Xu, D.W. Pang, L.N. Ji, Z.H. Lin, J. Electroanal. Chem. 600 (2007) 243.
[42] T. Sagara, M. Fukuda, N. Nakashima, J. Phys. Chem. B 102 (1998) 521.
[43] X.H. Zou, H. Li, G. Yang, H. Deng, J. Liu, R.H. Li, Q.L. Zhang, Y. Xiong, L.N. Ji, Inorg. Chem. 40 (2001) 7091.
[44] Q.X. Zhen, B.H. Ye, J.G. Liu, Chem. J. Chin. Univ. 20 (1999) 1661.
[45] H. Li, X.Y. Le, D.W. Pang, H. Deng, Z. Xu, Z.H. Lin, J. Inorg. Biochem. 99 (2005) 2240.
[46] T. Fukushima, E. Fujita, J.T. Muckerman, D.E. Polyansky, T. Wada, K. Tanaka, Inorg. Chem. 48 (2009) 11510.
[47] A.R. Hosseini, C.Y. Koh, J.D. Slinker, S. Flores-Torres, H.D. Abruña, G.G. Malliaras, Chem. Mater. 17 (2005) 6114.
[48] M.K. Brennman, T.J. Meyer, J.M. Papanikolas, J. Phys. Chem. A 109 (2004) 9938.